Biomass conversion into activated carbon as a sustainable energy material for the development of supercapacitor devices

by Rika Taslim

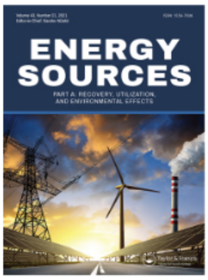

Energy Sources, Part A: Recovery, Utilization, and Environmental Effects

ISSN: (Print) (Online) Journal homepage: https://www.tandfonline.com/loi/ueso20

Biomass conversion into activated carbon as a sustainable energy material for the development of supercapacitor devices

Awitdrus Awitdrus, Deris Afdal Yusra, Erman Taer, Agustino Agustino, Apriwandi Apriwandi, Rakhmawati Farma & Rika Taslim

To cite this article: Awitdrus Awitdrus, Deris Afdal Yusra, Erman Taer, Agustino Agustino, Apriwandi Apriwandi, Rakhmawati Farma & Rika Taslim (2022) Biomass conversion into activated carbon as a sustainable energy material for the development of supercapacitor devices, Energy Sources, Part A: Recovery, Utilization, and Environmental Effects, 44:2, 3349-3359, DOI: 10.1080/15567036.2022.2064941

To link to this article: https://doi.org/10.1080/15567036.2022.2064941

Published online: 20 Apr 2022.

ENERGY SOURCES, PART A: RECOVERY, UTILIZATION, AND ENVIRONMENTAL EFFECTS
2022, VOL. 44, NO. 2, 3349–3359
https://doi.org/10.1080/15567036.2022.2064941

Taylor & Francis
Taylor & Francis Group

Biomass conversion into activated carbon as a sustainable energy material for the development of supercapacitor devices

Awitdrus Awitdrus[a], Deris Afdal Yusra[a], Erman Taer[a], Agustino Agustino[a], Apriwandi Apriwandi[a], Rakhmawati Farma[a], and Rika Taslim[b]

[a]Department of Physics, University of Riau, Simpang Baru, Indonesia; [b]Departement of Industrial Engineering, State Islamic University of Sultan Syarif Kasim, Simpang Baru, Indonesia

ABSTRACT

To address current energy consumption and chemical production, biomass is a promising alternative that can be used as an inexpensive and sustainable energy material for the development of supercapacitor devices. In this study, the jackfruit peel (JP) waste is used for the synthesis of an inexpensive and eco-friendly activated carbon (AC) as a sustainable energy material for the development of supercapacitor devices. JP wastes were synthesized by three-step approach consisting of KOH activation via nitrogen carbonization at 600°C and CO_2 activation at different temperatures (850, 900, and 950°C). The specific capacitances of supercapacitor cells are 85 F g^{-1}, 191 F g^{-1}, and 131 F g^{-1} for the JP-850, JP-900, and JP-950, respectively. Based on the results, the JP samples are suitable to be developed as an inexpensive and eco-friendly AC for electrode material in supercapacitor applications due to their good physicochemical properties and electrochemical performance.

ARTICLE HISTORY
Received 18 October 2021
Revised 06 April 2022
Accepted 07 April 2022

KEYWORDS
Jackfruit peel; activated carbon; sustainable energy material; three-step approach; supercapacitor

Introduction

Human welfare in this modern era is directly related to energy supply in the future. The availability of energy is a concern for all countries where the available sources are very limited. Nowadays, the renewable energy conversion and energy storage devices, i.e. batteries (Gou et al. 2019), fuel cells (Fan et al. 2018), and supercapacitors (Li and Xue 2014) need to be developed. Supercapacitors, also referred to as ultracapacitor, has gained regard as attractive candidates for new-generation energy storage systems, owing to their high specific power and specific energy (Yadav, Promila, and Hashmi 2020), rapid charge/discharge rates (Jain and Tripathi 2014), long life cycle (Guo et al. 2019), and eco-friendly nature (Wang et al. 2020).

Over the last few decades, activated carbon (AC) (Cheng et al. 2021), carbon nanofibers (CNFs) (Wang et al. 2021b), carbon nanotubes (CNTs) (Lv et al. 2021), carbon aerogel (Wu and Xu 2014; Yu, Li, and Wang 2017), and graphene (Fan et al. 2017; Vandana et al. 2020) have been studied and used as supercapacitor electrode materials. Among them, AC is regarded to be a promising electrode material because of its high specific surface area and many pore channels, which may contribute significantly to their high specific capacitance.

The use of AC from biomass materials for energy storage devices, especially supercapacitors, has attracted considerable attention. The design and development of carbon materials used as supercapacitor electrodes have an effect on the performance of these devices. The preparation of AC from biomass materials can be doneby chemical or physical activation process. As the synthesis of AC by chemical activation, biomass materials are treated with a chemical reagent (i.e. acids, alkaline, and salts) and followed by carbonization at 400–900 °C (Arvind and Hegde 2015). While the physical

CONTACT Awitdrus Awitdrus awitdrus@lecturer.unri.ac.id Department of Physics, University of Riau, Simpang Baru, Pekanbaru28293, Indonesia

activation process, biomass materials are carbonized and followed by activation at high temperature under an inert atmosphere or steam. Biomass-derived AC such as corn stalks (Awitdrus et al. 2018), *Cucumis melo* peel (Elaiyappillai et al. 2019), sakura (Ma et al. 2019), cocoa pods (Yetri et al. 2020a), pineapple leaf (Agustino et al. 2020), eucalyptus bark (Yadav, Promila, and Hashmi 2020), American poplar (Kumar et al. 2020), peanut shells (Jiang et al. 2020), laminaria japonica (Cheng et al. 2020), rotten potato (A. Wang et al. 2021), etc. have been widely used and demonstrated excellent candidates for use as supercapacitor electrode materials.

In addition, recent advances in AC from biomass for supercapacitors electrode materials have been reported. Sevilla et al. produced porous carbon from biomass-based products and was achieved the specific capacitance of 200 F g^{-1} in aqueous, 140 F g^{-1} in organic, and 160 F g^{-1} in ionic liquid electrolytes (Sevilla et al. 2019). Hérou and coworkers produce two materials from organosolv (OS) lignin and was achieved the specific capacitance of 210 F g^{-1} (Hérou et al. 2020). Furthermore, Yuan and groups have successfully fabricated biomass-based porous carbon for optimizing supercapacitor performance in an organic electrolyte (Yuan et al. 2020).

Jackfruit (*Artocarpus heterophyllus*) is commonly used for its pulp and seeds. Other parts such as the peels are unused and just thrown away so that they produce waste. The amount of this waste encourages us to utilize it as a source of AC for supercapacitor applications in order to increase the economic value of these wastes. In this study, we demonstrate the synthesis of an inexpensive and eco-friendly AC as a sustainable energy material for the development of supercapacitor devices. The synthesis of activated carbons from jackfruit peel (JP) waste by using KOH activation via nitrogen carbonization process in combination with subsequent CO_2 activation. As far as our knowledge, there are no studies on synthesis of JP waste AC using KOH activation via nitrogen carbonization and CO_2 activation have been reported, specifically for electrode material in supercapacitor devices. The novelty of this study is to develop an inexpensive and eco-friendly AC based on the three-step approach consisting of KOH activation via nitrogen carbonization at 600°C and CO_2 activation at different temperatures (850, 900, and 950°C), especially for supercapacitor electrode materials. The physico-chemical and electrochemical properties of the synthesized AC were investigated. This study has successfully demonstrated an inexpensive and eco-friendly AC as a sustainable energy material for the development of supercapacitor devices.

Experimental method

Preparations

The JP waste was collected from fruit traders in the traditional market, Riau Province, Indonesia. Initially, JP was cut transversely to the size of 5 cm and dried under sunlight for 3 d and followed by oven-dried for 2 d at 110°C. This material was pre-carbonization using an electric oven at 250°C with an increase of 50°C every 30 min. The pre-carbonized material was ground with a mortar and a ball mill for 20 h until the particle size achieved less than 53 μm. The fine powder was chemically activated using 0.5 M KOH, then followed by drying the sample in the oven for 48 h. The dried samples were printed to be pellets using a hydraulic press with a pressure of eight metrics tons as much as 20 pellets for each variation. The 20 pellets were carbonized under N_2 atmosphere at 600°C, while the CO_2 activation process at different temperatures (850°C, 900°C, and 950°C) for 2.5 h with a heating rate of 10°C min^{-1}. Finally, the AC was neutralized using distilled water until reached pH ~ 7 and then dried in the oven for 48 h. All the prepared samples were denoted as JP-850, JP-900, and JP-950, respectively.

Material characterization

Characterization of the physicochemical properties of JP samples includes density, surface morphology, elemental composition, crystallinity structure, and surface functionality. Surface morphology and elemental composition were observed by using SEM-EDS (JEOL-JSM 6510LA) and the crystallinity structure was characterized by using XRD (Shimadzu 7000) equipped with CuKα (λ = 0.1542 nm) radiation source. The surface functionality was characterized by using FTIR spectroscopy (IRPrestige-21, Shimadzu) with a scan range of 4800–450 cm^{-1}.

Electrochemical measurement

Electrochemical measurement was performed by a cyclic voltammetry method to determine the specific capacitance of supercapacitor cells. The supercapacitor cells from JP samples into sandwich form were made using teflon, current collector from stainless steel, separator using duck egg shell membrane, electrodes derived from JP, and 1 M H_2SO_4 electrolyte. This measurement was performed at voltage windows of 0–0.5 V with a scan rate of 1 mV s^{-1}. The specific capacitance, energy density, and power density were calculated by the equations (Hao et al. 2017; Zhao et al. 2015; Zhu et al. 2018):

$$C_{sp} = \frac{2I}{sm} \tag{1}$$

$$E = \frac{1}{7.2} CV^2 \tag{2}$$

$$P = 3600 \frac{E}{\Delta t} \tag{3}$$

where I (A) is the current, s (mV s^{-1}) is the scan rates, m (g) is the mass of the JP samples, V (V) is the cell voltage, and Δt (s) is the discharge time.

Results and discussion

Physicochemical properties analysis

Figure 1 displays the density of the JP samples before and after the carbonization and activation process. To determine the density of electrode, mass, diameter, and thickness of the electrodes were measured. The density data were calculated from 15 pellets for each variation. The densities of the JP-850, JP-900, and JP-950 before carbonization–activation are 1.065 g cm^{-3}, 1.115 g cm^{-3}, and 1.199 g cm^{-3}, with an average standard deviation of about 0.0334. The density of JP samples after the carbonization–activation process shows a linear decrease. This is influenced by the temperature

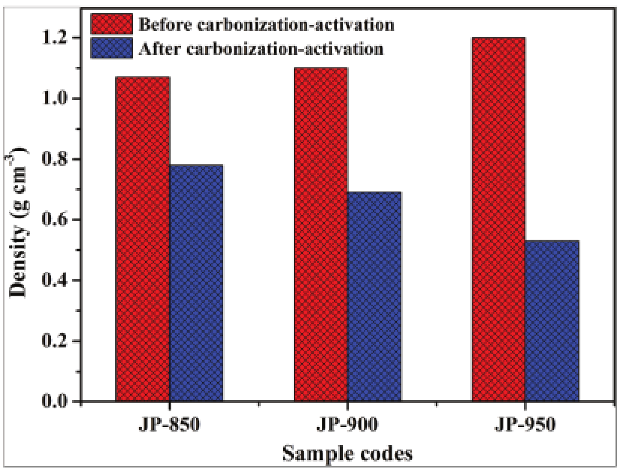

Figure 1. Density of the JP samples.

used in the CO_2 activation process. The densities of the JP-850, JP-900, and JP-950 before carbonization–activation are 0.774 g cm^{-3}, 0.675 g cm^{-3}, and 0.518 g cm^{-3}, with an average standard deviation of about 0.0429. The higher activation temperature results in lower density. The higher activation temperature could cause decomposition of complex compounds contained in the electrodes which underwent a process of evaporation; hence, new pores were formed on the electrode surfaces. The greatest decrease in density occurred in JP-950 samples as high as 0.681 g cm^{-3} with percentage about 56.79% and the smallest decrease occurred in JP-850 samples of 0.291 g cm^{-3} with percentage about 27.32%, respectively. This decrease is almost similar to other materials such as pineapple leaf fiber, which decreased by 27.93%–51.72% (Taer et al. 2021), and banana leaf, which decreased by 18.07–57.57% (Apriwandi et al. 2021).

Figure 2 represents the surface morphology of JP samples based on SEM micrograph. The SEM micrograph shows the presence of particles and fibers that have different length sizes for each sample. The micrograph of the surface of JP-850 sample (Figure 2a) shows a small number of fine particles and fine fibers. The visible fiber diameter is in the range of 56.83–153.46 nm. Figure 2b shows a micrograph of the surface with a lot of fine particles and fine fibers for JP-900 sample. The fiber looks very small with a fiber diameter in the range of 43.95–91.89 nm. As the temperature of CO_2 activation rises from 850°C to 900°C, the number of nanofibers increases while their diameter decreases. The micrograph of the surface of JP-950 sample (Figure 2c) shows a surface micrograph in the form of chunks of particles and large fibers that are different from other micrographs. The fibers have a diameter in the range of 49.03–95.52 nm. These fibers are also seen in various biomass waste have been previous studies, such as acacia leaves (Taer et al. 2020), *Aecha catechu* (Taer et al. 2019), pineapple leaf waste (Awitdrus et al. 2020), pineapple leaf fibers (Taer et al. 2021), etc.

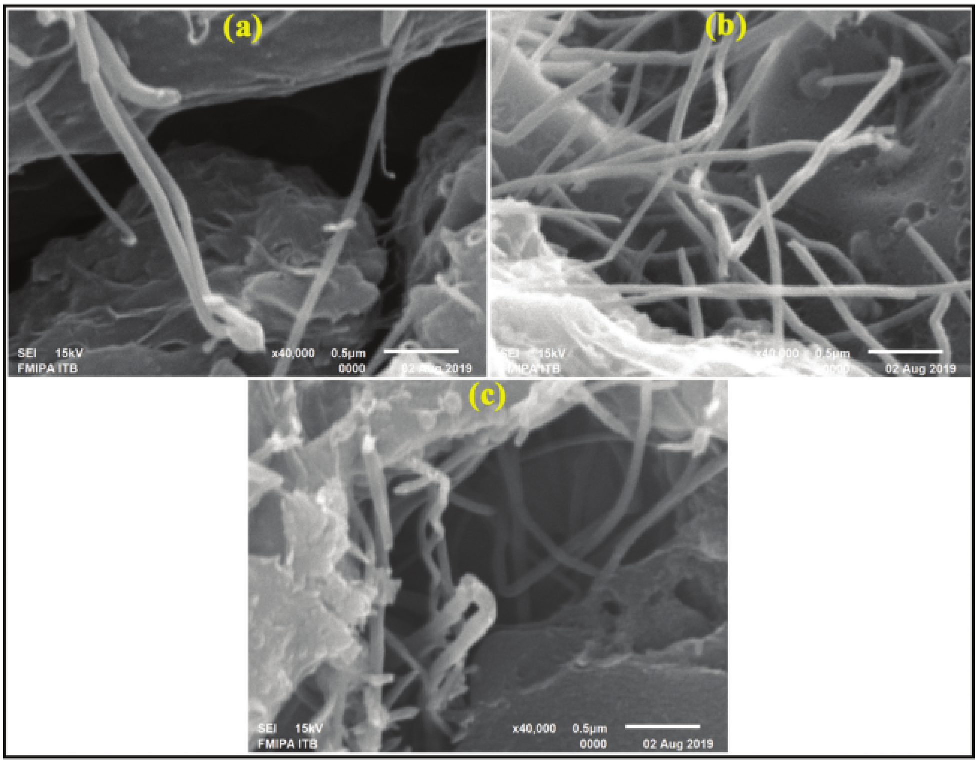

Figure 2. SEM micrographs of JP samples.

Table 1. Elements content of electrode from JP samples.

	JP-850	JP-900	JP-950
Elements		Atomic percentage	
Carbon	86.80	93.65	91.23
Oxygen	9.74	5.47	7.76
Magnesium	0.29	0.07	0.20
Silica	1.10	-	-
Potassium	0.83	0.44	0.16
Calcium	1.24	0.36	0.65

The elemental composition of the electrodes was observed using energy-dispersive X-ray spectroscopy. Table 1 shows the element contents in all samples. Carbon content on the surface of the JP sample was higher than the other elements. The highest carbon content is in the JP-900 sample with an atomic percentage of 93.65%. The high carbon content on the JP-900 sample also leads to a high specific capacitance. The decomposition process produces compounds that are volatile and detached from the element carbon, so that the carbon content in the sample is quite high.

Based on Table 1, the silica content is detected on the JP-850 sample with an atomic percentage of 1.10%, but the silica content is not detected on the JP-900 and JP-950 samples. This is due to an increase in the activation temperature from 850 up to 900 and 950°C, the silica content has evaporated at a higher temperature so that it's not detected in the EDS spectrum.

Figure 3 displays the XRD pattern of JP samples at different activation temperatures. The XRD pattern shows two broad peaks at around 22–24°, which are typical of the (002) plane reflection of the graphitized turbostratic carbon structure (Sodtipinta, Amornsakchai, and Pakawatpanurut 2017), and 43–45° which correspond to the (100) plane known as an characteristic of amorphous carbon structure

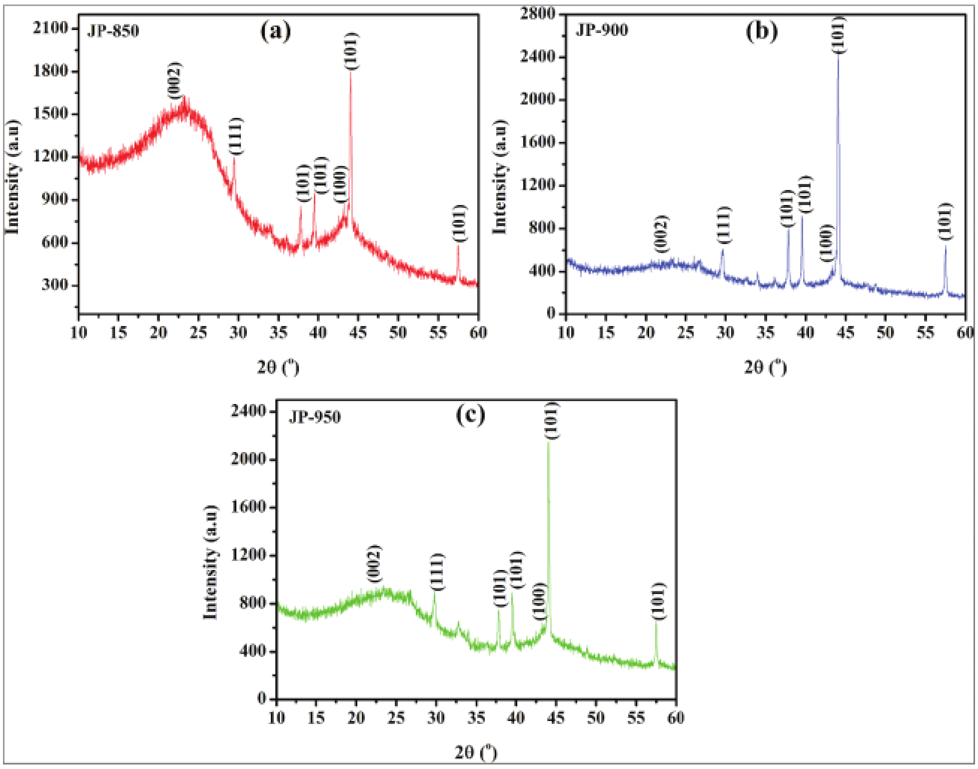

Figure 3. XRD patterns of (a) JP-850, (b) JP-900, and JP-950.

(Senthilkumar et al. 2011; Zhang and Zhang 2009). Moreover, the XRD pattern of all JP samples shows the existence of a peak of silica (SiO_2). It was can be seen that the JP900 and JP-950 samples show a high-intensity peak of silica rather than the JP-850 sample, this is due to the influence of activation temperature, where is the higher activation temperature causing silica content (SiO_2) to decompose easily so that the crystallinity properties of silica increase.

The interlayer distance (d_{002}), average crystallite thickness (L_c), and average graphene sheet diameter (L_a) are listed in Table 3. The interlayer distance (d_{002}) value was obtained from the 2θ degree of the (002) peak and showed the d_{002} value to be higher than d_{002} of graphite (0.335 nm). The interlayer distances of the JP samples are 0.370 nm, 0.390 nm, 0.381 nm, respectively. The lowest interlayer distance about of 0.370 nm was observed for JP-850 sample obtained in the activation temperature of 850°C. The highest interlayer distance about of 0.390 nm was observed for JP-900 sample obtained synthesized at the activation temperature of 900°C. As observed, these interlayer spacings are higher than the graphitic interplanar spacing for JP samples, the JP-900 sample showed a higher interlayer distance. The higher interlayer distance will facilitate easier penetration of electrolyte ions into electrode pores, which will further increase the specific capacitance. The L_c and L_a values were calculated using Scherer equations $L_{c,a} = \frac{K\lambda}{\beta_{002/100} \cos\theta_{002/100}}$, where L_c is the crystallite thickness (nm), L_a is the graphene sheet diameter (nm), K is the Scherer constant (0.9 for L_c and 1.84 for L_a), β is the FWHM of the (002) and (100) peaks, and θ is the angle in radians. The L_c values of the JP samples can be estimated to be 0.731–8.552 nm. The L_a values were within the range of 14.327–33.902 nm. The values listed in Table 2 confirm that the JP samples synthesized at 900°C show the highest interlayer spacing and the lowest L_c value.

Figure 4 displays the FTIR spectra of JP-850 and JP-900. Both of the samples show broadband positioned at 3520 cm^{-1}, which could be attributed to the -OH stretching in the hydroxyl group (Guo et al. 2019). The small band was observed located at 1450–1650 cm^{-1} which is corresponds to C=C stretching in aromatics. The small bands also observed at 550–1000 cm^{-1} correspond to C-H bending and stretching in out-of-plane in the benzene rings and could be indicated the formation of new C-H bonds during the activation process (Kan et al. 2015). Based on FTIR analysis, the functional groups compared from both samples, the activation temperature on the CO_2 activation process shows similar functional groups.

Table 2. The interlayer spacing (d_{hkl}), average crystallite thickness (L_c), and average graphene sheet diameter (L_a) of the JP samples.

	2θ, °		d, nm		L_c	L_a
Samples	(002)	(100)	(002)	(100)	(nm)	(nm)
JP-850	24.031	45.759	0.370	0.198	8.552	33.902
JP-900	22.765	43.802	0.390	0.207	0.731	14.896
JP-950	23.350	45.436	0.381	0.199	1.748	14.327

Table 3. The specific capacitance (C_{sp}), energy density (E), and power density (P) of the JP samples.

Activation temperature, °C	C_{sp}, F/g	E, Wh/kg	P, W/kg
850	85	2.95	21.28
900	191	6.62	47.97
950	131	4.55	32.83

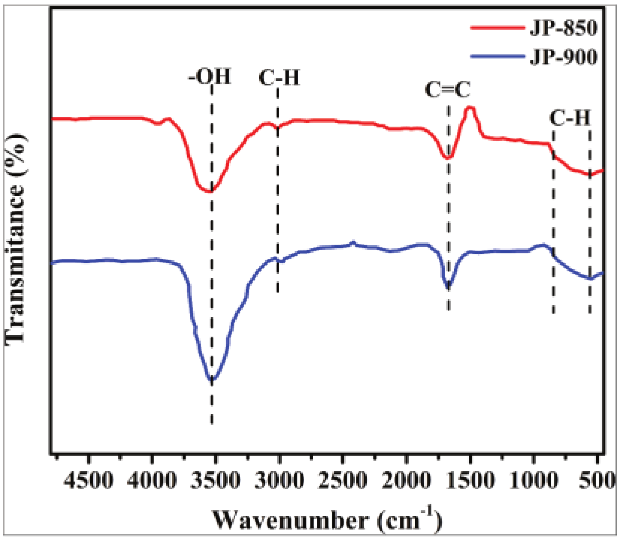

Figure 4. FTIR spectra of the JP-850 and JP-900.

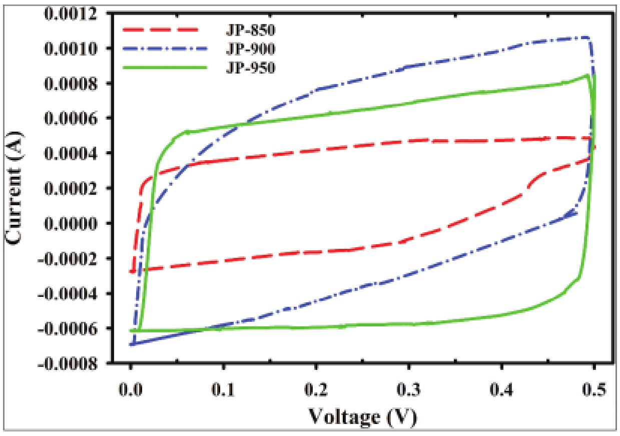

Figure 5. CV curves of the JP samples.

Electrochemical performance analysis

The electrochemical performance was evaluated by the cyclic voltammetry technique and shown in Figure 5. All the CV curves show an ideal shape of the carbon-based electrode, represented by a like rectangular shape which is indicating an ideal electrical double layer behavior. The large area of charge/discharge currents greatly affects the specific capacitance value, and the larger area of charging/discharging current produces the higher specific capacitance and vice versa. The specific capacitance of about 85 F g^{-1} was observed for JP-850 sample determined in activation temperature of 850°C. The rise in the activation temperature from 850°C to 900°C increases the specific capacitance from 85 F g^{-1} up to 191 F g^{-1}, with an increase of 124.71%. The rise in the activation temperature from 850°C to 900°C indicates a change in the distribution of nanofibers in the surface morphology of the sample which contributes to an increase in the specific capacitance. While the activation temperature rises to 950°C, the specific capacitance decreases by 31.41% to 131 F g^{-1}. This is due to the fact that at 950°C the physical structure of the electrode was damaged, which is characterized by a reduced distribution of nanofibers on the surface morphology of the sample as shown in the SEM analysis, thereby reducing its electrochemical performance. Based on this

Table 4. The electrochemical performance of the JP samples compared to other biomass at scan rate of 1 mV s^{-1}.

Biomass	Electrolyte	Cell configuration	Electrochemical measurement	C_{sp}, F/g	E, Wh/kg	P, W/kg	References
Banana fibers	1 M H_2SO_4	3-E	CV	156	63	5200	(Chaitra et al. 2017)
Coffee ground	2 M KOH	3-E	GCD	105	6.94	350	(Chiu and Lin 2019)
Cucumis melo fruit peel	1 M KOH	3-E	GCD	404	29.3	279.8	(Elaiyappillai et al. 2019)
Wood sawdust	6 M KOH	3-E	GCD	303	17.75	436	(Yang et al. 2019)
Cacao pods	1 M H_2SO_4	2-E	CV	140	-	-	(Yetri et al. 2020a)
Cacao peels	1 M H_2SO_4	2-E	CV	90	-	-	(Yetri et al. 2020b)
Hogweed stalks	1 M $DMP.BF_4$	2-E	GCD	114	-	-	(Tabarov et al. 2019)
Pine nut shells	1 M Na_2SO_4	2-E	GCD	52	23.45	450	(Qin et al. 2020)
Pineapple leaf	6 M KOH	2-E	CV	127	4.41	10.59	(Awitdrus et al. 2020)
Lumpy bracket	6 M KOH	2-E	GCD	223	-	-	(Serafin et al. 2019)
Tea waste	1 M Na_2SO_4	3-E	GCD	138	19.45	33,494.70	(Song et al. 2019)
Jackfruit peel	1 M H_2SO_4	2-E	CV	191	6.62	47.97	This work

analysis, the optimal temperature for the high performance of supercapacitor electrodes was found at 900°C. It was supported by SEM and EDS data, wherein the JP-900 sample has moredistribution of nanofibers on the surface morphology and also high carbon content compared to the JP-850 and JP-950 samples. The more distribution of nanofibers formed, the higher the electrode capacitance produced. In addition, the carbon electrode with nanofiber structure has an interconnected pore structure that can shorten the route for charge transport within the carbon electrode network, improve charge transfer efficiency, and reduce the internal resistance of the electrode (H. Wang et al. 2021).

The specific capacitance (C_{sp}), energy density (E), and power density (P) of the JP samples are listed in Table 3. Energy and power densities for JP samples are calculated using eEqs. (2) and (3). The JP-900 sample has a maximum energy density of 6.62 Wh kg^{-1} at a power density of 47.97 W kg^{-1}. In terms of energy and power densities, this value corresponds to the energy density and power density range of supercapacitors (Simon and Gogotsi 2008). Table 4 shows the electrochemical performance of the JP samples compared to other studies previously reported. The electrochemical performance of the JP samples is relatively higher in comparison to biomass-based AC has previously studied, such as banana fibers (Chaitra et al. 2017), coffee ground (Chiu and Lin 2019), cacao pods (Yetri et al. 2020a), pineapple leaf (Awitdrus et al. 2020), etc. The JP samples show great potential to be developed as an inexpensive and eco-friendly AC as an electrode material for supercapacitor devices.

Conclusions

In summary, we have successfully demonstrated the synthesis of an inexpensive and eco-friendly AC from JP waste as a sustainable energy material for the development of supercapacitor devices. The synthesis of ACs based on the three-step approach consisted of KOH activation via nitrogen carbonization at 600°C and CO_2 activation at different temperatures (850, 900, and 950°C). Based on SEM micrograph, the fiber diameter of the JP samples is 56.83–153.46 nm for JP-850, 3.95–91.89 nm for JP-850, and 49.03–95.52 for JP-850 nm. The JP-900 has an optimum specific capacitance of 191 F g^{-1} with an energy and power densities of 6.62 Wh kg^{-1} and 47.97 W kg^{-1}, respectively. Based on their electrochemical performance, the JP samples have good performance and are suitable to use as an electrode material for supercapacitor devices. To sum up, in terms of efficient utilization of raw materials and simple preparation process, this study has successfully demonstrated the synthesis of inexpensive and eco-friendly AC as a sustainable energy material for the development of supercapacitor devices.

Acknowledgments

The authors acknowledge the financial support from Kementerian Pendidikan, Kebudayaan, Riset, dan Teknologi through the third year of Basic research grant with contract no. 1418/UN.19.5.1.3/PT.01.03/2021 and the LPPM Universitas Riau through the project Bidang ilmu (Scientific research grant) with contract no. 662/UN.19.5.1.3/PT.01.03/2021.

Disclosure statement

No potential conflict of interest was reported by the author(s).

Funding

This work was supported by the Ministry of Education and Culture and Lembaga Penelitian dan Pengabdian Kepada Masyarakat Universitas Riau;

References

Agustino, A., Awitdrus, A., Amri, A., Taslim, R., Taer, E. 2020. The physical and electrochemical properties of activated carbon electrode derived from pineapple leaf waste for supercapacitor applications. *Journal of Physics. Conference Series* 1655 (1):012008-1-012008–7. doi:10.1088/1742-6596/1655/1/012008.

Apriwandi, A., E. Taer, R. Farma, R. N. Setiadi, and E. Amiruddin. 2021. A facile approach of micro-mesopores structure binder-free coin/monolith solid design activated carbon for electrode supercapacitor. *J Energy Storage* 40 (June):102823. doi:10.1016/j.est.2021.102823.

Arvind, D., and G. Hegde. 2015. Activated carbon nanospheres derived from bio-waste materials for supercapacitor applications - a review. *RSC Advances* 5 (107):88339–52. doi:10.1039/c5ra19392c.

Awitdrus, A. , Juliani, R., Taer, E., Farma, R., Iwantono, I., Deraman, M. 2018. Supercapacitor electrodes based on corn stalk binderless activated carbon. *Journal of Physics. Conference Series* 1120 (1):012005-1-012005–7. doi:10.1088/1742-6596/1120/1/012005.

Chaitra, K., T. R. Vinny, P. Sivaraman, N. Reddy, C. Hu, K. Venkatesh, S. C. Vivek, N. Nagaraju, and N. Kathyayini. 2017. KOH activated carbon derived from biomass-banana fibers as an efficient negative electrode in high performance asymmetric supercapacitor. *J Energy Chem* 26 (1):56–62. doi:10.1016/j.jechem.2016.07.003.

Cheng, J., S. C. Hu, G. T. Sun, K. Kang, M. Q. Zhu, and Z. C. Geng. 2021. Comparison of activated carbons prepared by one-step and two-step chemical activation process based on cotton stalk for supercapacitors application. *Energy* 215:119144. doi:10.1016/j.energy.2020.119144.

Cheng, Y., L. Wu, C. Fang, T. Li, J. Chen, M. Yang, and Q. Zhang. 2020. Synthesis of porous carbon materials derived from laminaria japonica via simple carbonization and activation for supercapacitors. *J Mater Res Technol* 9 (3):3261–71. doi:10.1016/j.jmrt.2020.01.022.

Chiu, Y. H., and L. Y. Lin. 2019. Effect of activating agents for producing activated carbon using a facile one-step synthesis with waste coffee grounds for symmetric supercapacitors. *Journal of the Taiwan Institute of Chemical Engineers* 101:77–85. doi:10.1016/j.jtice.2019.04.050.

Elaiyappillai, E., R. Srinivasan, Y. Johnbosco, P. Devakumar, K. Murugesan, K. Kesavan, and P. M. Johnson. 2019. Low cost activated carbon derived from Cucumis melo fruit peel for electrochemical supercapacitor application. *Applied Surface Science* 486 (May):527–38. doi:10.1016/j.apsusc.2019.05.004.

Fan, Y. M., W. L. Song, X. Li, and L. Z. Fan. 2017. Assembly of graphene aerogels into the 3D biomass-derived carbon frameworks on conductive substrates for flexible supercapacitors. *Carbon N Y* 111:658–66. doi:10.1016/j.carbon.2016.10.056.

Fan, L., B. Zhu, P. C. Su, and C. He. 2018. Nanomaterials and technologies for low temperature solid oxide fuel cells: Recent advances, challenges and opportunities. *Nano Energy* 45:148–76. doi:10.1016/j.nanoen.2017.12.044.

Gou, Q., C. Li, W. Zhong, X. Zhang, Q. Dong, and C. Lei. 2019. Hierarchical-structured porous N-doped carbon coating MnO microspheres with enhanced electrochemical performances as anode materials for lithium-ion batteries. *Electrochimica acta* 296:730–37. doi:10.1016/j.electacta.2018.11.104.

Guo, F., X. Jiang, X. Jia, S. Liang, L. Qian, and Z. Rao. 2019. Synthesis of biomass carbon electrode materials by bimetallic activation for the application in supercapacitors. *Journal of Electroanalytical Chemistry* 844 (May):105–15. doi:10.1016/j.jelechem.2019.05.004.

Hao, E., W. Liu, S. Liu, Y. Zhang, H. Wang, S. Chen, F. Cheng, S. Zhao, and H. Yang. 2017. Rich sulfur doped porous carbon materials derived from ginkgo leaves for multiple electrochemical energy storage devices. *J Mater Chem A* 5 (5):2204–14. doi:10.1039/C6TA08169J.

Hérou, S., M. Crespo Ribadeneyra, P. Schlee, H. Luo, L. C. Tanase, C. Roβberg, and M. Titirici. 2020. The impact of having an oxygen-rich microporous surface in carbon electrodes for high-power aqueous supercapacitors. *J Energy Chem* 53:36–48. doi:10.1016/j.jechem.2020.04.068.

Jain, A., and S. K. Tripathi. 2014. Fabrication and characterization of energy storing supercapacitor devices using coconut shell based activated charcoal electrode. *Mater Sci Eng B Solid-State Mater Adv Technol* 183 (1):54–60. doi:10.1016/j.mseb.2013.12.004.

Jiang, X., F. Guo, X. Jia, Y. Zhan, H. Zhou, and L. Qian. 2020. Synthesis of nitrogen-doped hierarchical porous carbons from peanut shell as a promising electrode material for high-performance supercapacitors. *J Energy Storage* 30 (January):101451. doi:10.1016/j.est.2020.101451.

Kan, Y., Q. Yue, J. Kong, B. Gao, and Q. Li. 2015. The application of activated carbon produced from waste printed circuit boards (PCBs) by H_3PO_4 and steam activation for the removal of malachite green. *Chem Eng J* 260:541–49. doi:10.1016/j.cej.2014.09.047.

Kumar, T. R., R. A. Senthil, Z. Pan, J. Pan, and Y. Sun. 2020. A tubular-like porous carbon derived from waste American poplar fruit as advanced electrode material for high-performance supercapacitor. *J Energy Storage* 32 (September):101903. doi:10.1016/j.est.2020.101903.

Li, M., and J. Xue. 2014. Integrated synthesis of nitrogen-doped mesoporous carbon from melamine resins with superior performance in supercapacitors. *The Journal of Physical Chemistry C* 118 (5):2507–17. doi:10.1021/jp410198r.

Lv, S., L. Ma, X. Shen, and H. Tong. 2021. One-step copper-catalyzed synthesis of porous carbon nanotubes for high-performance supercapacitors. *Microporous and Mesoporous Materials: The Official Journal of the International Zeolite Association* 310 (August 2020):110670. doi:10.1016/j.micromeso.2020.110670.

Ma, F., S. Ding, H. Ren, and Y. Liu. 2019. Sakura-based activated carbon preparation and its performance in supercapacitor applications. *RSC Advances* 9 (5):2474–83. doi:10.1039/c8ra09685f.

Qin, L., Z. Hou, S. Zhang, W. Zhang, and E. Jiang. 2020. Supercapacitive charge storage properties of porous carbons derived from pinenut shells. *Journal of Electroanalytical Chemistry* 866:114140. doi:10.1016/j.jelechem.2020.114140.

Senthilkumar, S. T., B. Senthilkumar, S. Balaji, C. Sanjeeviraja, and R. K. Selvan. 2011. Preparation of activated carbon from sorghum pith and its structural and electrochemical properties. *Materials Research Bulletin* 46 (3):413–19. doi:10.1016/j.materresbull.2010.12.002.

Serafin, J., M. Baca, M. Biegun, E. Mijowska, R. J. Kaleńczuk, J. Sreńscek-Nazzal, and B. Michalkiewicz. 2019. Direct conversion of biomass to nanoporous activated biocarbons for high CO_2 adsorption and supercapacitor applications. *Applied Surface Science* 497 (August):143722. doi:10.1016/j.apsusc.2019.143722.

Sevilla, M., N. Diez, G. A. Ferrero, and A. B. Fuertes. 2019. Sustainable supercapacitor electrodes produced by the activation of biomass with sodium thiosulfate. *Energy Storage Materials* 18:356–65. doi:10.1016/j.ensm.2019.01.023.

Simon, P., and Y. Gogotsi . 2008. Materials for electrochemical capacitors. *Nature Materials* 7 :845–54. doi:https://doi.org/10.1038/nmat2297 .

Sodtipinta, J., T. Amornsakchai, and P. Pakawatpanurut. 2017. Nanoporous carbon derived from agro-waste pineapple leaves for supercapacitor electrode. *Adv Nat Sci Nanosci Nanotechnol* 8 (3):1–10. doi:10.1088/2043-6254/aa7233.

Song, X., X. Ma, Y. Li, L. Ding, and R. Jiang. 2019. Tea waste derived microporous active carbon with enhanced double-layer supercapacitor behaviors. *Applied Surface Science* 487 (May):189–97. doi:10.1016/j.apsusc.2019.04.277.

Tabarov, F. S., M. V. Astakhov, A. T. Kalashnik, A. A. Klimont, I. S. Krechetov, and N. V. Isaeva. 2019. Micro-mesoporous carbon materials prepared from the hogweed (Heracleum) stalks as electrode materials for supercapacitors. *Russ J Electrochem* 55 (4):265–71. doi:10.1134/S1023193519020125.

Taer, E., A. Agustino, A. Awitdrus, R. Farma, and R. Taslim. 2021. The synthesis of carbon nanofiber derived from pineapple leaf fibers as a carbon electrode for supercapacitor application. *J Electrochem Energy Convers Storage* 18 (3):031004-1-031004–8. doi:10.1115/1.4048405.

Taer, E., R. Handayani, A. Apriwandi, R. Taslim, A. Awitdrus, A. Amun, A. Agustino, and I. Iwantono. 2019. The Synthesis of bridging carbon particles with carbon nanotubes from areca catechu husk waste as supercapacitor electrodes. *Int J Electrochem Sci* 14:9436–48. doi:10.20964/2019.10.34.

Taer, E., K. Natalia, A. Apriwandi, R. Taslim, A. Agustino, and R. Farma. 2020. The synthesis of activated carbon nanofiber electrode made from acacia leaves (Acacia mangium wild) as supercapacitors. *Adv Nat Sci Nanosci Nanotechnol* 11 (2):25007-1-25007–7. doi:10.1088/2043-6254/ab8b60.

Vandana, M., H. Vijeth, S. P. Ashokkumar, and H. Devendrappa. 2020. Effect of different gel electrolytes on conjugated polymer - graphene quantum dots based electrode for solid state hybrid supercapacitors. *Polym Technol Mater* 1–8. doi:10.1080/25740881.2020.1784221.

Wang, H., H. Niu, W. Hongjie, W. Wang, X. Jin, W. Hongxia, H. Zhou, and T. Lin. 2021b. Micro-meso porous structured carbon nanofibers with ultra-high surface area and large supercapacitor electrode capacitance. *Journal of Power Sources* 482 (August 2020):228986. doi:10.1016/j.jpowsour.2020.228986.

Wang, A., K. Sun, R. Xu, Y. Sun, and J. Jiang. 2021a. Cleanly synthesizing rotten potato-based activated carbon for supercapacitor by self-catalytic activation. *Journal of Cleaner Production* 283:125385. doi:10.1016/j.jclepro.2020.125385.

Wang, J., X. Zhang, Z. Li, Y. Ma, and L. Ma. 2020. Recent progress of biomass-derived carbon materials for supercapacitors. *Journal of Power Sources* 451 (October 2019):227794. doi:10.1016/j.jpowsour.2020.227794.

Wu, X. L., and A. W. Xu. 2014. Carbonaceous hydrogels and aerogels for supercapacitors. *J Mater Chem A* 2 (14):4852–64. doi:10.1039/c3ta13929h.

Yadav, N., R. Promila, and S. A. Hashmi. 2020. Hierarchical porous carbon derived from eucalyptus-bark as a sustainable electrode for high-performance solid-state supercapacitors. *Sustain Energy Fuels* 4 (4):1730–46. doi:10.1039/c9se00812h.

Yang, L., Y. Feng, M. Cao, and J. Yao. 2019. Two-step preparation of hierarchical porous carbon from KOH-activated wood sawdust for supercapacitor. *Materials Chemistry and Physics* 238 (May):121956. doi:10.1016/j.matchemphys.2019.121956.

Yetri, Y., A. T. Hoang, D. D. Mursida, T. E. Muldarisnur, and M. Q. Chau. 2020a. Synthesis of activated carbon monolith derived from cocoa pods for supercapacitor electrodes application. *Energy Sources, Part A Recover Util Environ Eff*:1–15. doi:10.1080/15567036.2020.1811433.

Yetri, Y., D. D. Mursida, E. Taer, and M. Agustino. 2020b. Identification of cacao peels potential as a basic of electrodes environmental friendly supercapacitors. *Key Engineering Materials* 846:274–81. 10.4028/www.scientific.net/KEM.846.274 .

Yu, M., J. Li, and L. Wang. 2017. KOH-activated carbon aerogels derived from sodium carboxymethyl cellulose for high-performance supercapacitors and dye adsorption. *Chem Eng J* 310:300–06. doi:10.1016/j.cej.2016.10.121.

Yuan, S., X. Huang, H. Wang, L. Xie, J. Cheng, Q. Kong, G. Sun, and C. M. Chen. 2020. Structure evolution of oxygen removal from porous carbon for optimizing supercapacitor performance. *J Energy Chem* 51:396–404. doi:10.1016/j.jechem.2020.04.004.

Zhang, G. Q., and S. T. Zhang. 2009. Characterization and electrochemical applications of a carbon with high density of surface functional groups produced from beer yeast. *Journal of Solid State Electrochemistry: Current Research and Development in Science and Technology* 13 (6):887–93. doi:10.1007/s10008-008-0623-2.

Zhao, J., H. Lai, Z. Lyu, Y. Jiang, K. Xie, X. Wang, Q. Wu, L. Yang, Z. Jin, Y. Ma, et al. 2015. Hydrophilic hierarchical nitrogen-doped carbon nanocages for ultrahigh supercapacitive performance. *Advanced Materials (Deerfield Beach, Fla.)* 27 (23):3541–45. doi:10.1002/adma.201500945.

Zhu, X., S. Yu, K. Xu, Y. Zhang, L. Zhang, G. Lou, Y. Wu, E. Zhu, H. Chen, Z. Shen, et al. 2018. Sustainable activated carbons from dead ginkgo leaves for supercapacitor electrode active materials. *Chemical Engineering Science* 181:36–45. doi:10.1016/j.ces.2018.02.004.

Biomass conversion into activated carbon as a sustainable energy material for the development of supercapacitor devices

ORIGINALITY REPORT

11%	7%	5%	3%
SIMILARITY INDEX	INTERNET SOURCES	PUBLICATIONS	STUDENT PAPERS

PRIMARY SOURCES

1	en.cnki.com.cn Internet Source	<1%
2	ijeas.akdeniz.edu.tr Internet Source	<1%
3	Mainara Generoso Faustino, Lucilena Rebelo Monteiro, Samia R. M. Lima, Tatiane B. S. C. da Silva et al. "Contamination characteristics in runoff fractions from a nuclear facility in São Paulo/Brazil", Research Square Platform LLC, 2022 Publication	<1%
4	Submitted to University of Hull Student Paper	<1%
5	converis.misis.ru Internet Source	<1%
6	docnum.univ-lorraine.fr Internet Source	<1%
7	jurnal.uns.ac.id Internet Source	<1%

8	mafiadoc.com Internet Source	<1 %
9	qspace.library.queensu.ca Internet Source	<1 %
10	sb-cris.nus.edu.sg Internet Source	<1 %
11	ui.adsabs.harvard.edu Internet Source	<1 %
12	www.owsd.net Internet Source	<1 %
13	Submitted to Chulalongkorn University Student Paper	<1 %
14	Jasso Flores Rosa Isela. "Efecto de la calidad y cantidad de la materia orgánica de tres especies arbóreas sobre la dinámica del carbono y nutrientes en un gradiente altitudinal de un bosque templado de alta montaña", TESIUNAM, 2020 Publication	<1 %
15	Nurul.Hazwani Aminuddin Rosli, Kam.Sheng Lau, Tan Winie, Siew.Xian Chin, Chin.Hua Chia. "Microwave-assisted reduction of graphene oxide for an electrochemical supercapacitor: structural and capacitance behavior", Materials Chemistry and Physics, 2021 Publication	<1 %
	Submitted to Thammasat University	

16	Student Paper	<1%
17	lib.buet.ac.bd:8080 Internet Source	<1%
18	Li, Xiaoguang, Zhikui Wang, Yunfeng Qiu, Qinmin Pan, and PingAn Hu. "3D graphene/ZnO nanorods composite networks as supercapacitor electrodes", Journal of Alloys and Compounds, 2015. Publication	<1%
19	Submitted to University of Edinburgh Student Paper	<1%
20	asianpubs.org Internet Source	<1%
21	esst.cip.com.cn Internet Source	<1%
22	librarysearch.aut.ac.nz Internet Source	<1%
23	profiles.murdoch.edu.au Internet Source	<1%
24	sigma-not.pl Internet Source	<1%
25	sinta.ristekbrin.go.id Internet Source	<1%
26	nur.nu.edu.kz Internet Source	<1%

27	www.chalmers.se Internet Source	<1 %
28	Embriz Pérez Geraldine. "Sistemas bioelectroquímicos para la producción de electricidad e hidrógeno a partir de aguas residuales", TESIUNAM, 2017 Publication	<1 %
29	Hapsoh, I R Dini, D Salbiah, S Tryana. " Application of biofertilizer consortium formulation of cellulolytic bacteria based on organic liquid waste on yield of upland rice (L.) ", IOP Conference Series: Earth and Environmental Science, 2020 Publication	<1 %
30	Honghong Yi, Hua Deng, Liping Yang, Xiao Long Tang, Qiongfen Yu, Zhiqing Ye. "Preparation of Activated Carbons from Tobacco Stems by Potassium Hydroxide Activation and Phosphine Adsorption", Separation Science and Technology, 2013 Publication	<1 %
31	Muhammad Imran Din, Rida Rehan. "Synthesis, Characterization, and Applications of Copper Nanoparticles", Analytical Letters, 2016 Publication	<1 %
32	Submitted to University of Malaya Student Paper	<1 %
33	Submitted to University of Surrey	

Student Paper

<1%

34 iehpc.gdut.edu.cn
Internet Source

<1%

35 123docz.net
Internet Source

<1%

36 Kaiqian Wang, Shuqiong Zhang, Yalin Cheng, Xinai Yu, Biyang Tu, Haisheng Tao. "Synthesis and electrochemical properties of coaxial-cable nanostructure carbon wrapped manganese oxide as anode for lithium ion batteries", Polyhedron, 2020
Publication

<1%

37 Hadi Mirzajani, Fariborz Mirlou, Emin Istif, Rahul Singh, Levent Beker. "Powering smart contact lenses for continuous health monitoring: Recent advancements and future challenges", Biosensors and Bioelectronics, 2021
Publication

<1%

38 Jungang Gao, Chaojie Jiang, Xiaohui Su. "Synthesis and Thermal Properties of Boron-Nitrogen Containing Phenol Formaldehyde Resin/MMT Nanocomposites", International Journal of Polymeric Materials, 2010
Publication

<1%

39 Sheila Hernandez, Juan V. Perales-Rondon, Aranzazu Heras, Alvaro Colina.

<1%

"Determination of uric acid in synthetic urine by using electrochemical surface oxidation enhanced Raman scattering", Analytica Chimica Acta, 2019
Publication

40	aimspress.com Internet Source	<1 %
41	electrochemsci.org Internet Source	<1 %
42	jscholarship.library.jhu.edu Internet Source	<1 %
43	Awitdrus, Rita Kartini Manulang, Agustino, Saktioto, Iwantono, Romi Fadli Syahputra, Rakhmawati Farma. "Effect of Chemical Activation on the Physical Properties of Activated Carbon from Banana Empty Fruit Bunches as Heavy Metal Adsorbent", Journal of Physics: Conference Series, 2020 Publication	<1 %
44	Chávez García Elizabeth. "Rehabilitación de suelos salino-sódicos para el establecimiento de una cobertura vegetal en el ex Lago de Texcoco", TESIUNAM, 2019 Publication	<1 %
45	Jyoti Jain, Shishir Sinha. "Potential of Pineapple Leaf Fibers and Their Modifications for Development of Tile Composites", Journal of Natural Fibers, 2021 Publication	<1 %

46	Mojtaba Azadi Aghdam, Hamid-Reza Kariminia, Sedigheh Safari. "Removal of lignin, COD, and color from pulp and paper wastewater using electrocoagulation", Desalination and Water Treatment, 2015 Publication	<1 %
47	Yanzhen Liu, Yongfeng Li, Ming Zhong, Yonggang Yang, Yuefang Wen, Maozhang Wang. "A green and ultrafast approach to the synthesis of scalable graphene nanosheets with Zn powder for electrochemical energy storage", Journal of Materials Chemistry, 2011 Publication	<1 %
48	Z. Sun, H. Yuan, Z. Liu, B. Han, X. Zhang. "A Highly Efficient Chemical Sensor Material for H2S: α-Fe2O3 Nanotubes Fabricated Using Carbon Nanotube Templates", Advanced Materials, 2005 Publication	<1 %
49	cers.ejournal.unri.ac.id Internet Source	<1 %
50	js.vnu.edu.vn Internet Source	<1 %
51	research.aalto.fi Internet Source	<1 %
52	research.chalmers.se Internet Source	<1 %

53	www.ije.ir Internet Source	<1 %
54	www.journals.elsevier.com Internet Source	<1 %
55	www.wjgnet.com Internet Source	<1 %
56	L. Vayssieres, C. Sathe, S. M. Butorin, D. K. Shuh, J. Nordgren, J. Guo. "One-Dimensional Quantum-Confinement Effect in α-Fe2O3 Ultrafine Nanorod Arrays", Advanced Materials, 2005 Publication	<1 %
57	R.A. Boschi, D.R. Salahub. "The far ultra-violet spectra of some branched chain iodo-alkanes, iodo-cyclo-alkanes, fluoro-iodo-alkanes and iodo-alkenes", Molecular Physics, 1972 Publication	<1 %
58	Senthilkumar, S.T.. "Preparation of activated carbon from sorghum pith and its structural and electrochemical properties", Materials Research Bulletin, 201103 Publication	<1 %

Exclude quotes	Off	Exclude matches	Off
Exclude bibliography	Off		